Pflügers Arch – Eur J Physiol (1999) 437:523–528

ORIGINAL ARTICLE

Francisco J. Urbano · Osvaldo D. Uchitel

L-Type calcium channels unmasked by cell-permeant Ca^{2+} buffer at mouse motor nerve terminals

Received: 2 September 1998 / Received after revision:13 October 1998 / Accepted:14 October 1998

Abstract The involvement of the different types of voltage-dependent calcium channels (VDCC) in both DM-BAPTA-AM-incubated and EGTA-AM-incubated mature mice levator auris neuromuscular junctions (NMJ) was studied. We evaluated the effects of ω-agatoxin IVA (ω-Aga IVA), nitrendipine and ω-conotoxin GVIA (ω-CgTX) (P/Q-, L- and N-type VDCC blockers, respectively) on perineurial calcium currents (I_{Ca}) and nerve-evoked transmitter release. The application of ω-Aga IVA (100 nM) drastically reduced perineurial I_{Ca} (>90%) and nerve-evoked transmitter release (>90% of reduction in quantal content, *m)* at both DM-BAPTA-AM-incubated and EGTA-AM-incubated NMJ. The L-type VDCC antagonist nitrendipine (10 µM) caused a significant reduction (23±9%, *n*=5) of perineurial I_{Ca} at DM-BAPTA-AM-incubated NMJ. In addition, after the block of P/Q-type VDCC with ω-Aga IVA (100 nM), nitrendipine reduced (>90%, *n*=2) the remaining perineurial I_{Ca}. Such reduction was not observed at EGTA-AM-incubated NMJ, before or after the total block of P/Q-type VDCC. Moreover, nitrendipine did not significantly reduce the quantal content of DM-BAPTA-AM-incubated NMJ. Finally, the application of ω-CgTX (5 µM) did not significantly affect perineurial I_{Ca} or nerve-evoked transmitter release at either DM-BAPTA-AM-incubated or EGTA-AM-incubated NMJ. These results show the existence of a nitrendipine-sensitive, L-type component of perineurial I_{Ca} in DM-BAPTA-AM-incubated NMJ of mature mice.

F.J. Urbano · O.D. Uchitel
Laboratorio de Fisiología y Biología Molecular (LFBM),
Departamento de Ciencias Biológicas,
Facultad de Ciencias Exactas y Naturales,
Universidad de Buenos Aires, Ciudad Universitaria,
Pebellón II-2do piso, 1428-Buenos Aires, Argentina

O.D. Uchitel (✉)
Laboratorio de Fisiología y Biología Molecular (LFBM),
Departamento de Ciencias Biológicas,
Ciudad Universitaria, Pabellón II,
2do piso, 1428-Buenos Aires, Argentina
e-mail: ODU@BG.FCEN.UBA.AR
Tel.: +54-1-7886954, Fax: +54-1-7802788

Key words Calcium channel · Cell-permeant calcium buffers · DM-BAPTA-AM · EGTA-AM · Neuromuscular junction

Introduction

The influx of Ca^{2+} through voltage-dependent calcium channels (VDCC) at nerve terminals is the link between an action potential and transmitter release [2, 18]. At mature mammalian neuromuscular junctions (NMJ), neurotransmitter release is mediated by VDCC of the P/Q-type family, on the basis of the blocking effects of both funnel-web spider toxin (FTX) and ω-agatoxin IVA (ω-Aga IVA) on electrically evoked and K^+-evoked acetylcholine (ACh) release and presynaptic Ca^{2+} currents [6, 14, 29, 37, 38]. In contrast, neither the L- nor the N-type VDCC have been found to participate in the evoked release of ACh in these mature termini [5, 6, 27, 31]. Some of this pharmacological evidence has been reinforced using immunocytochemical techniques [7, 26].

The function of the VDCC is controlled by voltage as well as by Ca^{2+}-dependent inactivation, the later being mediated by the Ca^{2+} influx through the channel [23]. This provides an intrinsic feedback mechanism through changes of the intracellular Ca^{2+} concentration ($[Ca^{2+}]_i$), which modulates both the magnitude and the duration of Ca^{2+} entry through VDCC. Both enzymatic and nonenzymatic mechanisms have been proposed to mediate the process of Ca^{2+}-dependent inactivation of VDCC in a variety of cell types. In particular, Ca^{2+}-dependent inhibition of the L-type VDCC has been described as a complex mechanism, where the Ca^{2+} is thought to bind directly to the channel protein [11, 13, 16, 17] as well as to a regulatory protein [12, 32] to promote inactivation.

The intracellular injection of Ca^{2+} buffers has been used to study Ca^{2+}-dependent inactivation phenomena in several systems [23]. BAPTA and EGTA buffers, which are those most used, have similar affinity constants for Ca^{2+} (i.e. K_D values). But EGTA has a binding rate constant (i.e. k_{on}) for Ca^{2+} greater than 100 times slower [1].

In addition, the cell-permeant acetoxymethylester (AM) forms of these buffers have been accepted as a noninvasive way to control the $[Ca^{2+}]_i$ [30, 34–36]. Furthermore, the fastest BAPTA-derived buffers (e.g. DM-BAPTA) have been used to reduce the rapid rise in $[Ca^{2+}]_i$ at the vicinity of the VDCC pore [33], and also to make inferences about the spatial relationship between Ca^{2+} influx through VDCC and neurotransmitter release [25].

Thus, the objective of the present study was to investigate whether intracellular Ca^{2+} buffers are able to affect the pharmacological profile of the perineurial calcium currents (I_{Ca}) and nerve-evoked transmission release of mature mouse NMJ. We found the existence of a nitrendipine-sensitive, L-type component of perineurial I_{Ca} in NMJ of mature mice incubated in 5′-dimethyl-1,2-bis(2-aminophenoxy)ethane-*N*,*N*,*N*′,*N*′-tetraacetoxymethyl ester (DM-BAPTA-AM).

Materials and methods

Experiments were carried out on the levator auris longus muscle of male Swiss mice weighting 20–30 g. The animals were cared for in accordance with national guidelines for the humane treatment of laboratory animals, which are as protective as those of the US National Institutes of Health. Animals were anaesthetized with an overdose of 2% tribromoethanol (0.15 ml per 10 g body mass, intraperitoneally). The corresponding muscle with its nerve supply was excised and dissected on a Sylgard-coated Petri dish containing a physiological saline solution of the following composition (mM): NaCl, 137; KCl, 5; $CaCl_2$, 2; $MgSO_4$, 1; $NaHCO_3$, 12; Na_2HPO_4, 1 and glucose 11; continuously bubbled with 95% O_2/5% CO_2. The preparation was then transferred to a recording chamber of 1.5 ml. Experiments were performed at room temperature (20–23°C).

Values are expressed as means±SEM. Statistical significance (*P* values in the text and figure legends) was evaluated by two-tailed Student's *t* test (for unpaired values and not assuming equal variances).

Electrophysiological recordings

Evoked endplate potentials (EPPs) and miniature endplate potentials (MEPPs) were recorded intracellularly with conventional glass microelectrodes filled with 3 M KCl (10–15 MΩ resistance). During the recording of EPPs muscle contraction was prevented by d-tubocurarine (dTC; 0.8–1.2 µM). After impalement of a muscle fibre, the nerve was stimulated continuously for 1 min at 0.5 Hz, using two platinum electrodes coupled to a pulse generator associated with a stimulus isolation unit, and then 100 successive EPP were recorded (minimum 15 fibres per NMJ). The mean quantal content (*m*) of the evoked response was evaluated by the coefficient of variation method, calculated as:

$$m=(V_{EPP})^2/[(S_{EPP})^2-(S_{noise})^2]$$

where V_{EPP} is the mean amplitude of the EPP, and S_{EPP} and S_{noise} are the standard deviations of the recorded EPP amplitudes and of the noise, respectively [15].

MEPPs were recorded for periods of 1–2 min and stored on tape for further analysis. For evaluating K^+-evoked MEPPs, frequency was always evaluated after 30 min of incubating the muscle with a modified saline solution where the [KCl] was increased from 5 to 10 mM. The iso-osmolarity was maintained by adjusting $[Na^+]_o$. In both cases, MEPPs frequency was computer analysed (Axoscope 1.0, Axon Instruments).

Presynaptic I_{Ca}

Presynaptic currents were recorded extracellularly upon stimulation of the motor nerve by means of glass microelectrodes filled with 2M NaCl (5–10 MΩ) inserted into the perineurial sheath of small-diameter nerve bundles [22]. In all the experiments, control and toxin-treated records were obtained without changing the position of the electrode and once a stable recording had been achieved. Presynaptic I_{Ca} were obtained by adding tetraethylammonium (TEA; 10 mM), 3,4-diaminopyridine (DAP; 250 µM) and dTC (30 µM). The recording electrodes were connected to an Axoclamp-2A amplifier (Axon Instruments). A distant Ag-AgCl electrode connected to the bath solution via an agar bridge (3.5% agar in 137 mM NaCl) was used as reference. The signals were digitized (TL-1 DMA interface; Axon Instruments), stored and computer analysed. The percentage block was measured by integrals of the Cd^{2+}-sensitive, upward deflection (see Fig. 4), corresponding to the Ca^{2+} influx (I_{Ca}) from the terminal [22].

Loading procedure

The preparation was incubated with the AM forms of buffers for 2 h at 37°C in Ca^{2+}-free saline solution in the presence of 10 µM of the AM forms of buffers. Control experiments were performed incubating with the final concentration of dimethylsulphoxide (DMSO). After incubation, the preparations were first washed for 15 min with the Ca^{2+}-free solution and finally for 15 min with normal physiological saline solution.

Facilitation of transmitter release

Facilitation of transmitter release was studied using intracellular microelectrodes under conditions of low probability of release (modified saline solution containing 0.5 mM Ca^{2+} and 5 mM Mg^{2+}). Transmitter release was elicited by nerve stimulation through an isolation unit coupled to a computer. Then, 15 trains of stimuli at 100 Hz were applied every 10 s and the facilitation index was estimated as:

$$I_f=[(Amp_9+Amp_{10})/2]/Amp_1$$

where Amp_9 and Amp_{10} are the average amplitudes of the 9th and 10th endplate potentials (EPPs) of the train and Amp_1 is the mean average of the first EPP [30, 34]. I_f values were obtained before and after incubating the preparation with both DM-BAPTA-AM and ethylene glycol-bis-(β-aminoethylether)-*N*,*N*,*N*′,*N*′-tetraacetoxymethyl ester (EGTA-AM).

Toxins and chemicals

Tribromoethanol was purchased from Aldrich. Nitrendipine was purchased from Research Biochemicals. dTC, DAP and all other salts were of analytical grade and purchased from Sigma (St. Louis, Mo., USA). DM-BAPTA-AM and EGTA-AM were purchased from Molecular Probes. The synthetic polypeptides ω-conotoxin GVIA (ω-CgTx) and ω-Aga IVA were purchased from Alomone Laboratories (Jerusalem, Israel). In all cases, both control and toxin-treated fibres were assayed in the presence of 0.01% BSA (Sigma).

Nitrendipine was made up as a 50 mM stock solution in ethanol, stored at 4°C and protected from light. Experiments in the presence of nitrendipine were carried out in the absence of direct illumination. The final ethanol concentration in control and drug-treated preparations was 0.1% (v/v). In control experiments this concentration of ethanol did not affect any of the parameters under study (*n*=2, data not shown).

DM-BAPTA-AM and EGTA-AM were prepared as 10 mM stock solutions dissolved in DMSO and stored in a freezer at –20°C. Aliquots were diluted in the incubation solution to yield the final concentration of 10 µM. Neither the incubation nor the DMSO affected any of the parameters under study (*n*=5, data not shown)

Administration of nitrendipine was performed during constant flow perfusion (≅2 ml/min). Toxins (ω-CgTX and ω-Aga IVA) and $CdCl_2$ (100 µM) were added directly to the bath after stopped the perfusion and having obtained stable recordings for at least 15 min.

Results

Loading of cell-permeant Ca^{2+} buffers into incubated NMJ

Initially, in order to verify the loading of the AM forms, facilitation of transmitter release was studied after incubation with both cell-permeant Ca^{2+} buffers. After incubation with DM-BAPTA-AM, but not EGTA-AM, a significant decrease of the I_f of transmitter release was continually observed throughout the experiments (n=3; data not shown), as previously described [30].

However, it was also important to verify the loading of EGTA-AM. In this sense, Losavio and Muchnik [20] have recently described an EGTA-AM-mediated reduction of MEPP frequency in rat NMJ. Then, it was of interest to study whether both cell-permeant Ca^{2+} buffers reduce spontaneous and/or K^+-evoked MEPP frequency compared with control conditions (i.e. DMSO-incubated NMJ) at mouse NMJ.

Figure 1A,B shows the MEPP frequency recorded in DMSO-, DM-BAPTA-AM- and EGTA-AM-incubated NMJ (empty, filled and hatched bars, respectively), bathed with normal (5 mM K^+) and 10 mM K^+ physiological saline solution, respectively. The spontaneous MEPP frequency (Fig. 1A) was not significantly different under these conditions (DMSO, 49.0±4.8 min^{-1}; DM-BAPTA-AM, 42.5±6.9 min^{-1}; EGTA-AM, 43.5±7.8 min^{-1}; P>0.5, n=8). Nevertheless, the K^+-evoked MEPP frequency (Fig. 1B) was drastically decreased at both DM-BAPTA-AM- and EGTA-AM-incubated NMJ (DMSO, 125.5±8.7 min^{-1}; DM-BAPTA-AM, 60.9±4.9 min^{-1}; EGTA-AM, 67.5±3.0 min^{-1}; P<0.001, n=8). Moreover, no significant differences were observed comparing the K^+-evoked MEPP frequency of DM-BAPTA-AM- and EGTA-AM-incubated NMJ (P>0.7).

These data suggest the normal loading of both cell-permeant Ca^{2+} buffers and the continuous presence of the active salt forms of the buffers at incubated NMJ.

Effects of Ca^{2+} channel blockers on perineurial I_{Ca} currents in incubated NMJ

Perineurial I_{Ca} signals of DMSO-, DM-BAPTA-AM- and EGTA-AM-incubated NMJ recorded in the presence of dTC (30 µM), TEA (10 mM) and DAP (250 µM) showed initially the capacitative artefact, followed by downward and upward deflections. Here, the downward component reflects the Na^+ entry in the last heminodes, while the upward deflection corresponds to the Ca^{2+} influx (I_{Ca}) from the terminal [22]. In all cases, the I_{Ca} was suppressed after the bath application of Cd^{2+} (100 µM; see Fig. 4D).

The application of 5 µM ω-CgTX (n=4), at a concentration that ensures maximal blocking effects in other systems, did not produce any change in the *perineurial* I_{Ca} of either DM-BAPTA-AM or EGTA-AM-incubated NMJ (Fig. 2A).

At both DM-BAPTA-AM- and EGTA-AM-incubated NMJ, the application of 100 nM ω-Aga IVA drastically blocked the perineurial I_{Ca} (Fig. 2B). Washing the prepa-

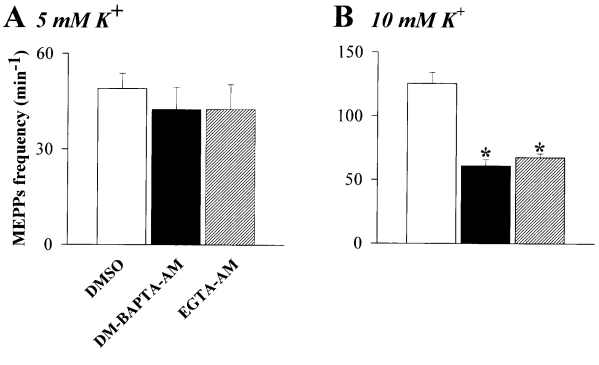

Fig. 1 **A** Spontaneous (*5 mM K^+*) miniature end-plate potential (*MEPP*) frequency (DMSO-incubated; *empty bar*) was not significantly reduced after incubation with neither DM-BAPTA-AM (*filled bar*) or EGTA-AM (*hatched bar*). **B** Bar diagram showing that K^+-evoked (*10 mM K^+*) MEPP frequency (DMSO-incubated; *empty bar*) was significantly reduced after incubation with both DM-BAPTA-AM (*filled bar*) and EGTA-AM (*hatched bar*). *P<0.001 compared with value in 10 mM K^+ of the DMSO-incubated neuromuscular junction (*NMJ*). Each *bar* represents the mean ±SEM of at least 15 fibres per NMJ (n=12). [*DM-BAPTA-AM* 5′-Dimethyl-1,2-bis(2-aminophenoxy)ethane-*N,N,N′,N′*-tetraacetoxymethyl ester, *EGTA-AM* ethylene glycol-bis-(β-aminoethylether)-*N,N,N′,N′*-tetraacetoxymethyl ester]

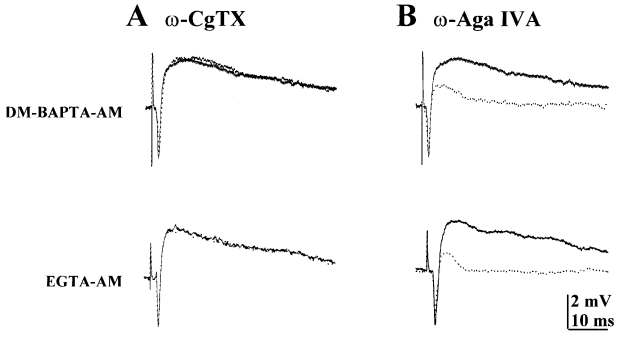

Fig. 2A, B Effect of Ca^{2+} channels blockers ω-conotoxin GVIA (*ω-CgTX*) and ω-agatoxin IVA (*ω-Aga IVA*) on perineurial I_{Ca} of both DM-BAPTA-AM-incubated and EGTA-AM-incubated NMJ. **A** Superimposed recordings from the same site before (*continuous line*) and 30 min after addition of 5 µM ω-CgTX (*dotted line*) from a DM-BAPTA-AM-incubated (*upper panel*) and an EGTA-AM-incubated (*lower panel)* NMJ. **B** Superimposed recordings from the same site before (*continuous line*) and 30 min after addition of 100 nM ω-Aga IVA (*dotted line*) from a DM-BAPTA-AM-incubated (*upper panel*) and an EGTA-AM-incubated (*lower panel*) NMJ. All currents were recorded in the presence of d-tubocurarine (*dTC*, 30 µM), tetraethylammonium (*TEA*, 10 mM) and 3,4-diaminopyridine (*DAP*, 250 µM) and are the average of three currents elicited by nerve stimulation every 30 s. Each *panel* corresponds to different preparations

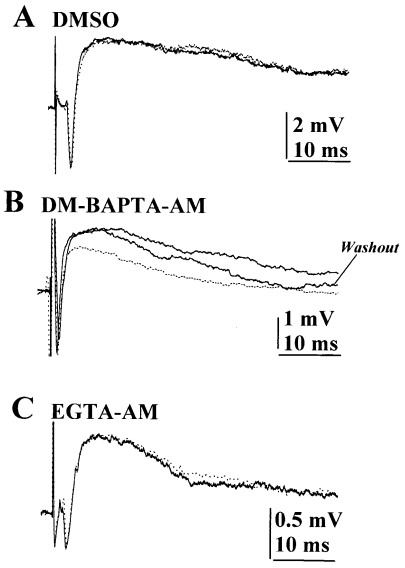

Fig. 3A–C Effects of nitrendipine on the presynaptic perineurial I_{Ca} of DMSO-, DM-BAPTA-AM- and EGTA-AM-incubated NMJ. **A** Superimposed recordings from the same site before (*continuous line*) and 40 min after perfusion with 10 µM nitrendipine (*dotted line*) from a DMSO-incubated NMJ. **B** Superimposed recordings from the same site before (*continuous line*), 40 min after perfusion with 10 µM nitrendipine (*dotted line*) and 30 min of washout (*washout*) from a DM-BAPTA-AM-incubated NMJ. **C** Same as **A**, but for an EGTA-AM-incubated NMJ. Note that *traces* are superimposed on both DMSO- and EGTA-AM-incubated NMJ, indicating that nitrendipine has no effect on I_{Ca}. All currents were recorded in the presence of dTC (30 µM), TEA (10 mM) and DAP (250 µM) and are the average of three currents elicited by nerve stimulation every 30 s. **A–C** Data are from different preparations

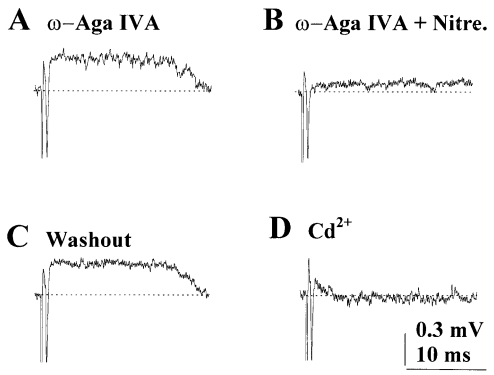

Fig. 4 Superimposed recordings from the same site 40 min after addition of 100 nM ω-Aga IVA to the bath (**A**), 45 min after perfusion with 10 µM nitrendipine (**B**) and after 30 min of washout (**C**) from a DM-BAPTA-AM-incubated NMJ. Note that after washout the application of 100 µM Cd^{2+} (**D**) abolished the remnant I_{Ca}, which indicates the Ca^{2+}-mediated nature of the nitrendipine-blocked I_{Ca}. All currents were recorded in the presence of dTC (30 µM), TEA (10 mM) and DAP (250 µM) and are the average of four currents elicited by nerve stimulation every 30 s. **A–D** Data are from the same preparation

ration with toxin-free solution could not reverse the blocking effects of this drug (data not shown). The averaged block of ω-Aga IVA (100 nM) was 90±4% and 89±3% for DM-BAPTA-AM- and EGTA-AM- incubated NMJ, respectively (n=5).

Thus, the strong inhibition provoked by ω-Aga IVA and the lack of effect of ω-CgTX suggested that activation of presynaptic P/Q-type VDCC is responsible for the major part of perineurial I_{Ca} of incubated NMJ.

The application of 10 µM nitrendipine did not produce any change in the perineurial I_{Ca} of DMSO-incubated NMJ (n=4, Fig. 3A). However, the application of nitrendipine (10 µM) to the DM-BAPTA-AM-incubated NMJ partially reduced the perineurial I_{Ca}. Figure 3B illustrates the effects of the application of 10 µM nitrendipine (dotted line) on the perineurial I_{Ca} recorded in a DM-BAPTA-AM-incubated NMJ. Note that this blocking effect of nitrendipine was partially reversible (see Fig. 3B). The averaged block observed was 23±9% (n=5). Nevertheless, the application of 10 µM nitrendipine did not affect (n=4) the perineurial I_{Ca} at EGTA-AM-incubated NMJ (Fig. 3C).

Furthermore, the blocking effect of nitrendipine was also observed after the application of 100 nM ω-Aga IVA to DM-BAPTA-AM-incubated NMJ (Fig. 4). Indeed, the application of nitrendipine (10 µM) practically abolished the remaining I_{Ca} (Fig. 4B) in a reversible way (Fig. 4C), after the application of ω-Aga IVA. However, at both DMSO- and EGTA-AM-incubated NMJ, after the application of ω-Aga IVA (100 nM), the remaining I_{Ca} was not sensitive to nitrendipine (n=4; data not shown).

Thus, these results reveal the existence of a nitrendipine-sensitive, L-type component of perineurial I_{Ca} in DM-BAPTA-AM-incubated NMJ of mature mice.

Effects of nitrendipine on nerve-evoked release in DM-BAPTA-AM-incubated NMJ

In order to evaluate if the nitrendipine-sensitive component of presynaptic I_{Ca} described above participates in

Table 1 Effect of calcium channels blockers ω-Aga IVA and nifedipine on quantal content (m) of both DMSO- and DM-BAPTA-AM-incubated NMJ. Each *value* represents the mean ±SEM

	Control	Nitrendipine (10 µM)	ω-Aga IVA (100 nM)
DMSO	94.5±10.9 (n=2 NMJ; 32 fibres)	–	<10* (n=1 NMJ; 28 fibres)
DM-BAPTA-AM	91.9±8.8** (n=2 NMJ; 35 fibres)	99.0±11.8*** (n=2 NMJ; 30 fibres)	<10* (n=1 NMJ; 33 fibres)

*P<0.05 versus before the toxin in each condition
**Not significant versus DMSO-incubated NMJ
***Not significant versus DM-BAPTA-AM-incubated NMJ

the release process at DM-BAPTA-AM-incubated NMJ, we tested the effects of 10 μM nitrendipine on quantal content (*m*).

The estimated *m* values for DMSO- and DM-BAPTA-AM-incubated NMJ, before and after the application of 10 μM nitrendipine, are expressed in Table 1.

Hence, nitrendipine did not affect significantly the quantal content of the DM-BAPTA-AM-incubated NMJ (see Table 1).

On the other hand, in DMSO- and DM-BAPTA-AM-incubated NMJ, ω-Aga IVA (100 nM) drastically reduced *m* (see Table 1). Also, nitrendipine had no further effects on the quantal content of the DM-BAPTA-AM-incubated NMJ after the application of 100 nM ω-Aga IVA (n=2, data not shown).

Discussion

It is well known that once in the cell, and after the action of cytoplasmic esterases, cell-permeant Ca^{2+} buffers do become active intracellular Ca^{2+} buffers [35]. Under our conditions of incubation (2 h at 37°C) and according to Tymianski et al. [36], the highest intracellular concentration of DM-BAPTA and EGTA may have been reached. The intracellular buffers normally regulate the $[Ca^{2+}]_i$ around their K_D values (K_D estimated by Pethig et al. [28] to be 150 and 210 nM for DM-BAPTA and EGTA, respectively); therefore, the resting $[Ca^{2+}]_i$ during our experiments should be in the nanomolar range for both DM-BAPTA- and EGTA-loaded NMJ. Moreover, DM-BAPTA has a binding rate constant (i.e. k_{on}) more than 100 times higher than that of EGTA [1]. Thus, the observed reduction in K^+-evoked MEPP frequency could be explained by the buffering response of both buffers to the massive Ca^{2+} entry from the extracellular space after the K^+-mediated tonic depolarization of the NMJ. In contrast, the reduction of I_f observed specifically with DM-BAPTA-AM relies on its k_{on} rather on the K_D. Thus, the data indicate that both buffers were successfully loaded. In addition, other authors have also described analogous effects of cell-permeant buffers on K^+-evoked MEPP frequency at rat NMJ [20] and on the I_f at NMJ of frog [34] and mouse [30].

Indeed, in our experiments DM-BAPTA-AM did not significantly change the quantal content of the incubated NMJ (see Table 1). However, BAPTA, but not EGTA, was able to reduce the evoked transmitter release when injected into the presynaptic terminal of the squid giant synapse [1]. This might be due to differences in spatial vesicle and/or Ca^{2+} distribution in squid versus mammalian NMJ.

The results presented here show that ω-Aga IVA but not ω-CgTX drastically reduced perineurial I_{Ca} and nerve-evoked transmitter release at both DM-BAPTA-AM- and EGTA-AM-incubated NMJ. This indicates that the P/Q- but not the N-type VDCC mediates transmission release under these experimental conditions, in agreement with previous results in studies of mature mice [6, 14, 29, 31, 37, 38].

The absence of a blocking effect of nitrendipine (10 μM) observed at both DMSO- and EGTA-AM-incubated NMJ as well as the presence of a nitrendipine-sensitive, L-type component of the I_{Ca} at DM-BAPTA-AM-incubated NMJ suggests that only the fast intracellular buffer was able to unmask it.

The existence of a blocking effect of nitrendipine after application of ω-Aga IVA (100 nM) to DM-BAPTA-AM-incubated NMJ, but not to DMSO- or EGTA-AM-incubated NMJ suggests that the Ca^{2+} influx through the P/Q-type is not involved in the inactivation process of these channels. In this way, other authors have described that the Ca^{2+} influx through L-type channels can selectively facilitate the inactivation of other adjacent L-type channels, without a generalized elevation of bulk $[Ca^{2+}]_i$ [16]. Thus, our observation of the nitrendipine-sensitive, L-type component of I_{Ca} only when a fast intracellular buffer is used suggests a rapid action of intracellular DM-BAPTA, regulating the Ca^{2+} inflow through these channels.

Nevertheless, the application of nitrendipine did not affect the quantal content of DM-BAPTA-AM-incubated NMJ, before or after the application of ω-Aga IVA, suggesting that this nitrendipine-sensitive L-type component of presynaptic I_{Ca} is not directly implicated in nerve-evoked transmitter release. Although this lack of effect of dihydropyridines in nerve-evoked release at mature NMJ has been previously reported [5, 27], other roles for the VDCC present in nerve terminals have been recently described. In this sense, the Ca^{2+} entering through VDCC present in the axons can play an important role in regulating action potential propagation [21]. Furthermore, in hippocampal neurons the Ca^{2+} influx through L-type VDCC is able to cause the translocation of calmodulin from the cytoplasm to the nucleus, whereas that through other VDCC types is not [8]. This translocation of calmodulin provides a form of cellular communication that combines the specificity of local Ca^{2+} signalling with the ability to produce action at a distance. Likewise, the L-type VDCC has also been implicated in gene expression, mediating the synaptic activation of immediate early genes [24]. This suggests that the L-type VDCC could participate in more complex reactions in which local and short-lived signals are transcribed into long-lasting global signals [25].

The regulation of VDCC by Ca^{2+} is not yet clear: Ca^{2+} ions could be acting by binding directly to the channel [11, 13, 16, 17] or via a protein phosphatase-mediated dephosphorylation process [32]. In this sense, Arenson and Gill [4] have recently described that protein phosphorylation and dephosphorylation may regulate the activity of L-type channels at frog NMJ. Then, the L-type VDCC present at mature mouse NMJ could be regulated by Ca^{2+}-dependent enzymatic mechanisms.

Also, as judged by the effects of dihydropyridines, the presence of the L-type VDCC may also be regulated during both development and reinnervation of the vertebrates [3, 10, 19] and amphibian [9] NMJ.

In conclusion, these results provide evidence for a nitrendipine-sensitive, L-type component of perineurial I_{Ca},

unmasked by the fast intracellular buffer DM-BAPTA, which is not involved in nerve-evoked transmitter release. Further studies should be done in order to deduce the physiological functions of these VDCC.

Acknowledgements We wish to thank Dr. Cristina R. Artalejo, Dr. Eleonora Katz, Lic. Marcelo Rosato-Siri and Lic. Rafael Depetris for reading the manuscript and discussions. We also like to thank Dr. N. Saccomano of Pfizer for generously providing the toxin ω-Aga IVA. This work was supported by the Muscular Dystrophy Association, UBA (ME 064) and CONICET (PICT 0310). Dr. Francisco J. Urbano is a Dr. M. Morales Foundation (Tazacorte. Canary Islands. Spain) postdoctoral fellow.

References

1. Adler EM, Augustine GF, Duffy SN, Charlton MP (1991) Alien intracellular calcium chelators attenuate neurotransmitter release at the squid synapse. J Neurosci 11:1496–1507
2. Agustine GJ, Charlton MP, Smith SJ (1987) Calcium action in synaptic transmitter release. Annu Rev Neurosci 10:633–693
3. Angelov DN, Neiss WF, Streppel M, Andermahr J, Mader K, Stennert E (1996) Nimodipine accelerates axonal sprouting after surgical repair of rat facial nerve. J Neurosci 16:1041–1048
4. Arenson MS, Gill DS (1996) Differential effects of an L-type Ca^{2+} channel antagonist on activity- and phosphorylation-enhanced release of acetylcholine at the neuromuscular junction of the frog *in vitro*. Eur J Neurosci 8:437–445
5. Atchison WD (1989) Dihydropyridine-sensitive and -insensitive components of acetylcholine release from rat motor nerve terminals. J Pharmacol Exp Ther 251:672–678
6. Bowersox SS, Miljanich GP, Sugiura Y, Li C, Nadasdi L, Hoffman BB, Ramachandran J, Ko C-P (1995) Differential blockade of voltage-sensitive calcium channels at the mouse neuromuscular junction by novel ω-conopeptides and ω-agatoxin-IVA. J Pharmacol Exp Ther 273:248–256
7. Day NC, Wood SJ, Ince PG, Volsen SG, Smith W, Slater CR, Shaw PJ (1997) Differential localization of voltage-dependent calcium channel α_1 subunits at the human and rat neuromuscular junction. J Neurosci 17:6226–6235
8. Deisseroth K, Heist EK, Tsien RW (1998) Translocation of calmodulin to the nucleus supports CREB phosphorylation in hippocampal neurons. Nature 392:198–202
9. Fu W-M, Huang F-L (1994) L-Type Ca^{2+} channel is involved in the regulation of spontaneous transmitter release at developing neuromuscular synapses. Neuroscience 58:131–140
10. Gray DB, Brusés JL, Pilar GR (1992) Developmental switch in the pharmacology of Ca^{2+} channels coupled to acetylcholine release. Neuron 8:1–20
11. Haack JA, Rosenberg RL (1994) Calcium-dependent inactivation of L-type calcium channels in planar lipid bilayers. Biophys J 66:1051–1060
12. Hirano Y, Hiraoka M (1994) dual modulation of unitary L-type Ca^{2+} channel currents by $[Ca^{2+}]_i$ in fura-2-loaded guinea-pig ventricular myocytes. J Physiol (Lond) 480:449–463
13. Höfer GF, Hohenthanner K, Baumgartner W, Groschner K, Klugbauer N, Hofmann F, Romanin C (1997) Intracellular Ca^{2+} inactivates L-type Ca^{2+} channels with Hill coefficient of ≅1 and an inhibition constant of ≅4 μM by reducing channel's open probability. Biophys J 73:1857–1865
14. Hong SJ, Chang CC (1995) Inhibition of acetylcholine release from mouse motor nerve by a P-type calcium channel blocker, ω-agatoxin IVA. J Physiol (Lond) 482:283–290
15. Hubbard JI, Llinás R, Quastel DML (1969) Electrophysiological analysis of synaptic transmission. Edward Arnold, London
16. Imredy JP, Yue DT (1992) Submicroscopic Ca^{2+} diffusion mediates inhibitory coupling between individual Ca^{2+} channels. Neuron 9:197–207
17. Imredy JP, Yue DT (1994) Mechanism of Ca^{2+}-sensitive inactivation of L-type Ca^{2+} channels. Neuron 12:1301–1318
18. Katz B, Miledi R (1970) Further study of the role of calcium in synaptic transmission. J Physiol (Lond) 207:789–801
19. Katz E, Ferro PA, Weisz G, Uchitel OD (1996) Calcium channels involved in synaptic transmission at the mature and regenerating mouse neuromuscular junction. J Physiol (Lond) 497: 687–697
20. Losavio A, Muchnik S (1997) Spontaneous acetylcholine release in mammalian neuromuscular junctions. Am J Physiol 273:C1835–C1841
21. Lüscher C, Lipp P, Lüscher H–R, Niggli E (1996) Control of action potential propagation by intracellular Ca^{2+} in cultured rat dorsal root ganglion cells. J Physiol (Lond) 490:319–324.
22. Mallart A (1985) Electric current flow inside perineurial sheaths of mouse motor nerves. J Physiol (Lond) 368:565–575
23. McDonald TF, Pelzer S, Trautwein W, Pelzer DJ (1994) Regulation and modulation of calcium channels in cardiac, skeletal, and smooth muscle cells. Physiol Rev 74:365–507
24. Murphy TH, Worley PF, Baraban JM (1991) L-Type voltage-sensitive channels mediate synaptic activation of immediate early genes. Neuron 7:625–635
25. Neher E (1998) Vesicle pools and Ca^{2+} microdomains: new tools for understanding their roles in neurotransmitter release. Neuron 20:389–399
26. Ousley AH, Froehner SC (1994) An anti-peptide antibody specific for the class A calcium channel alpha 1 subunit labels mammalian neuromuscular junction. Proc Natl Acad Sci USA 91:12263–12267
27. Penner R, Dreyer F (1986) Two different presynaptic calcium currents in mouse motor nerve terminals. Pflügers Arch 406: 190–197
28. Pethig R, Kuhn M, Payne R, Adler E, Chen T-H, Jaffe LF (1989) On the dissociation constants of BAPTA-type calcium buffers. Cell Calcium 10:491–498
29. Protti DA, Uchitel OD (1993) Transmitter release and presynaptic Ca^{2+} currents blocked by the spider toxin ω-Aga-IVA. Neuroreport 5:333–336
30. Protti DA, Uchitel OD (1997) P/Q-type calcium channels activate neighbouring calcium-dependent potassium channels in mouse motor nerve terminals. Pflügers Arch 434:406–412
31. Protti DA, Szczupak L, Scornik FS, Uchitel OD (1991) Effect of ω-conotoxin GVIA on neurotransmitter releases at the mouse neuromuscular junction. Brain Res 557:336–339
32. Schuhmann K, Romanin C, Baumgartner W, Groschner K (1997) Intracellular Ca^{2+} inhibits smooth muscle L-type Ca^{2+} channels by activation of protein phosphatase type 2B and direct interaction with the channel. J Gen Physiol 110:503–513
33. Stern MD (1992) Buffering of calcium in the vicinity of a channel pore. Cell Calcium 13:183–192
34. Tanabe N, Kijima H (1992) Ca^{2+}-dependent and independent components of transmitter release at the frog neuromuscular junction. J Physiol (Lond) 455:271–289
35. Tsien RY (1981) A non-disruptive technique for loading calcium buffers and indicators into cells. Nature 290:527–528
36. Tymianski M, Charlton MP, Carlen PL, Tator CH (1994) Properties of neuroprotective cell-permeant Ca^{2+} chelators: effects on $[Ca^{2+}]_i$ and glutamate neurotoxicity in vitro. J Neurophysiol 72:1973–1992
37. Uchitel OD, Protti DA, Sánchez V, Cherksey BD, Sugimori M, Llinás R (1992) P-type voltage-dependent calcium channel mediates presynaptic calcium influx and transmitter release in mammalian synapses. Proc Natl Acad Sci USA 89:3330–3333
38. Xu Y-F, Atchinson WD (1996) Effects of ω-agatoxin-IVA and ω-conotoxin-MVIIC on perineurial Ca^{2+} and Ca^{2+}-activated K^+ currents of mouse motor nerve terminals. J Pharmacol Exp Ther 279:1229–1236